Temperature-mediated growth of single-walled carbon-nanotube intramolecular junctions

YAGANG YAO[1], QINGWEN LI[2], JIN ZHANG[1]*, RAN LIU[1], LIYING JIAO[1], YUNTIAN T. ZHU[2] AND ZHONGFAN LIU[1]*

[1]Centre for Nanoscale Science and Technology (CNST), Beijing National Laboratory for Molecular Sciences (BNLMS), State Key Laboratory for Structural Chemistry of Unstable and Stable Species, Key Laboratory for the Physics and Chemistry of Nanodevices, College of Chemistry and Molecular Engineering, Peking University, Beijing 100871, PR China

[2]Los Alamos National Laboratory, Los Alamos, New Mexico 87545, USA

*e-mail: jinzhang@pku.edu.cn; zfliu@pku.edu.cn

Published online: 18 March 2007; doi:10.1038/nmat1865

Single-walled carbon nanotubes (SWNTs) possess superior electronic and physical properties that make them ideal candidates for making next-generation electronic circuits that break the size limitation of current silicon-based technology[1–4]. The first critical step in making a full SWNT electronic circuit is to make SWNT intramolecular junctions in a controlled manner. Although SWNT intramolecular junctions have been grown by several methods[2,5–8], they only grew inadvertently in most cases. Here, we report well-controlled temperature-mediated growth of intramolecular junctions in SWNTs. Specifically, by changing the temperature during growth, we found that SWNTs systematically form intramolecular junctions. This was achieved by a consistent variation in the SWNT diameter and chirality with changing growth temperature even though the catalyst particles remained the same. These findings provide a potential approach for growing SWNT intramolecular junctions at desired locations, sizes and orientations, which are important for making SWNT electronic circuits.

Figure 1 shows single-walled carbon-nanotube (SWNT) intramolecular junctions formed by changing the growth temperature from $T_1 = 900\,^{\circ}\mathrm{C}$ to $T_2 = 950\,^{\circ}\mathrm{C}$ (Fig. 1a,c,e), and from $T_1 = 950\,^{\circ}\mathrm{C}$ to $T_2 = 900\,^{\circ}\mathrm{C}$ (Fig. 1b,d,f) during catalytic chemical vapour deposition (CVD) of ethanol[9–11]. The detailed growth process is shown in Supplementary Information, part I. Briefly, a 0.01 M catalyst solution of $FeCl_3$ or $CoCl_2$ was applied to one edge of a substrate by microcontact printing. The ethanol vapour was introduced into the furnace by bubbling 200 s.c.c.m. Ar through the ethanol. The growth rate of the SWNTs in our CVD system was around $5\,\mu\mathrm{m\,s^{-1}}$. In the figure, the SWNTs grew from left to right following the gas flow direction. The diameter evolution along individual ultralong SWNTs was characterized using a micro-Raman spectroscope (Renishaw 1000) coupled with a confocal imaging microscope, with an excitation energy of 1.96 eV (632.8 nm) and a 1 μm excitation spot size. The diameters of individual nanotubes were estimated using the equation: $d = 248\,\mathrm{cm^{-1}}/\omega_{\mathrm{RBM}}$, where ω_{RBM} is the radial-breathing-mode frequency, which was derived for SWNTs on silicon substrates[12]. As shown in Fig. 1a,c,e, when the growth temperature was increased from $T_1 = 900\,^{\circ}\mathrm{C}$ to $T_2 = 950\,^{\circ}\mathrm{C}$, Raman mapping along a SWNT detected a sharp RBM shift from 137.1 to $143.0\,\mathrm{cm^{-1}}$, which corresponds to a diameter change from 1.81 to 1.73 nm. In other words, the diameter of the SWNT decreased by around 4% across the transition. For convenience, the transition position is marked as 0 in Fig. 1c. In addition, the G_+ and G_- peaks shifted from $1{,}592.0\,\mathrm{cm^{-1}}$ and $1{,}576.3\,\mathrm{cm^{-1}}$ to $1{,}586.7\,\mathrm{cm^{-1}}$ and $1{,}572.1\,\mathrm{cm^{-1}}$, respectively, but did not change shape, suggesting that the SWNT remained semiconductive across the transition. We randomly mapped three individual SWNTs, all of which showed an RBM shift that corresponded to a decrease in diameter.

It is well known that the diameter (d) of a SWNT is related to its chirality (specified by (n, m)), which can be described as

$$d = 0.249\sqrt{n^2 + m^2 + nm}/\pi.$$

Using this equation and resonant Raman theory[13], we found that the chirality of the SWNT in Fig. 1a,c,e was (14, 12) at T_1 (ref. 14), and it changed to (20, 3) at T_2 after the transition. SWNTs with different chiralities will exhibit different bandgaps and therefore different electronic behaviours[15]. As a result, the introduction of a diameter transition on a single nanotube generates an intramolecular junction. Figure 1e indicates the formation of a semiconductor–semiconductor (S–S) junction.

Figure 1b,d,f shows that an abrupt temperature decrease from $T_1 = 950\,^{\circ}\mathrm{C}$ to $T_2 = 900\,^{\circ}\mathrm{C}$ induced an intramolecular junction in a SWNT. As shown in Fig. 1d, the RBM shifted from 208.6 to $186.6\,\mathrm{cm^{-1}}$, corresponding to a diameter increase from 1.19 to 1.33 nm. This diameter variation can also be confirmed by atomic force microscopy (AFM) data (see Supplementary Information, Fig. S4 for details). The G-band—which appeared as two peaks at $1{,}542.3\,\mathrm{cm^{-1}}$ and $1{,}586.4\,\mathrm{cm^{-1}}$, and moved forming three peaks at $1{,}561.2\,\mathrm{cm^{-1}}$, $1{,}576.7\,\mathrm{cm^{-1}}$ and $1{,}607.4\,\mathrm{cm^{-1}}$ (see Fig. 1f)—indicates that the junction was metallic–metallic (M–M) type. Raman mappings of three randomly selected individual SWNTs consistently revealed intramolecular junctions formed by an increase in diameter.

To verify the repeatability of the formation of intramolecular junctions induced by a change in temperature, we oscillated the temperature between 950 and 880 °C three times (see Fig. 2a). Each

©2007 Nature Publishing Group

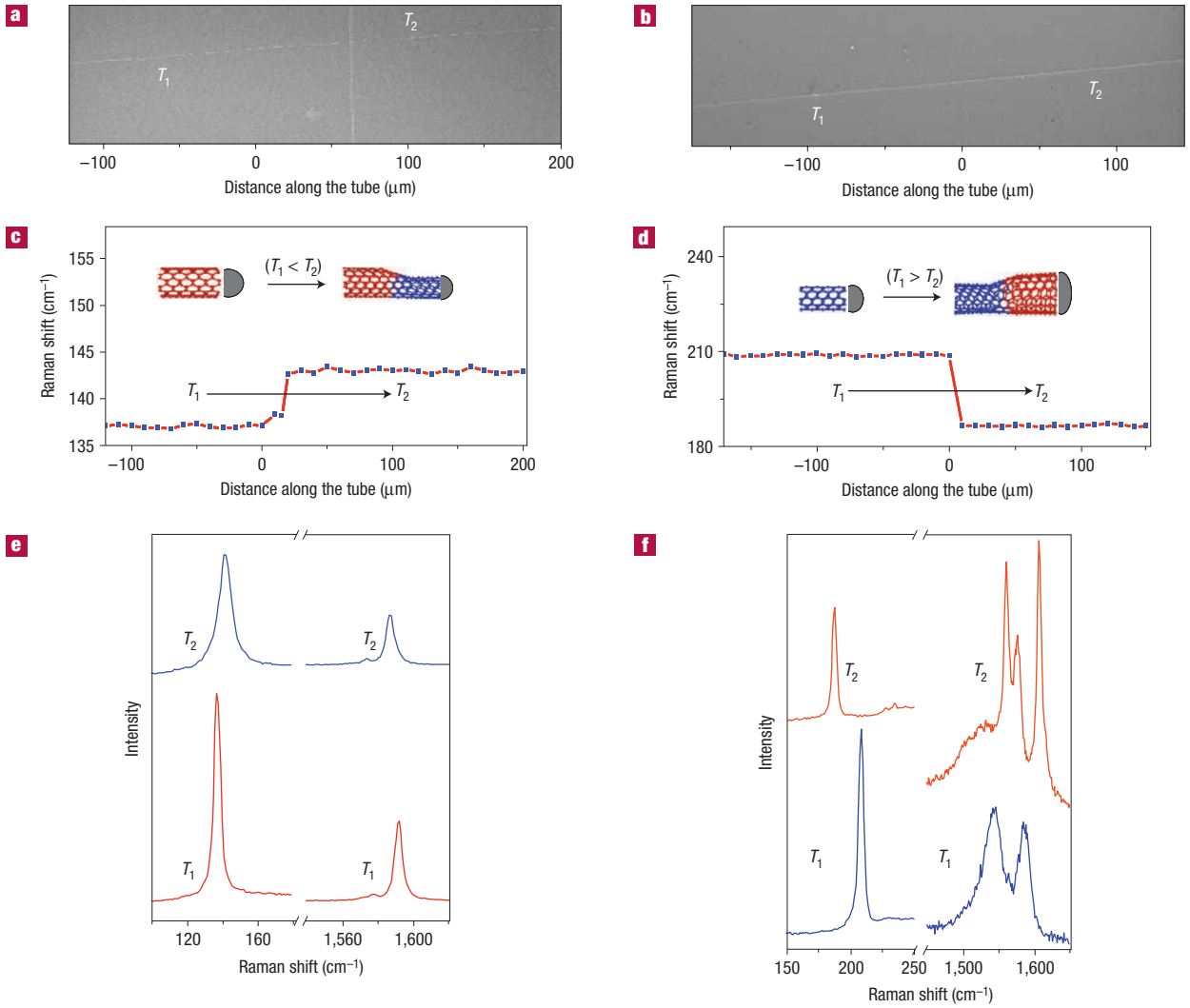

Figure 1 Intramolecular junctions induced by a change in temperature during CVD. a,**b**, Scanning electron microscopy (Hitachi S-4800) images of a SWNT junction induced by an increase in temperature from 900 to 950 °C (**a**) and a SWNT junction induced by a decrease in temperature from 950 to 900 °C (**b**). The vertical line in **a** is the mark on the patterned substrate that was used to locate the SWNTs. The zero on the horizontal axes of **a** and **b** refers to the identified positions of the intramolecular junctions. **c**,**d**, The shift of the Raman RBM peak along the SWNT in **a** (**c**) and along the SWNT in **b** (**d**) with a junction at location 0. Insets: Schematic diagrams of the SWNT diameter variation with temperature at the junction[20]. **e**,**f**, Raman-RBM-peak and G-peak shift between the SWNT segments grown at $T_1 = 900$ °C and $T_2 = 950$ °C, respectively (**e**) and between the SWNT segments grown at $T_1 = 950$ °C and $T_2 = 900$ °C, respectively (**f**).

oscillation involved cooling from 950 to 880 °C in 20 s and then heating back to 950 °C in 40 s. Individual SWNTs grown during this process are shown in Fig. 2c. RBM spectra corresponding to different time–temperature points in Fig. 2a are shown in Fig. 2b. Clearly, the RBM peak position oscillated following the temperature oscillation. In other words, six intramolecular junctions were formed. This demonstrates that it is possible to form arrays of intramolecular junctions using temperature control.

The above results indicate that varying the temperature can be used as an effective method to tune the diameter and generate intramolecular junctions along SWNTs. For this method to work reliably, the diameters of individual SWNTs should stay uniform when grown under a constant temperature. We mapped a few dozen SWNTs grown under a constant temperature of 950 °C and found that their diameters indeed stayed uniform along their length, which is consistent with a previous study[9]. For example, Raman scanning along a 6-mm-long SWNT revealed that the RBM peak is positioned at 137.2 cm^{-1}, with a variation of less than 0.4% (see Supplementary Information, Fig. S1). In other words, the diameter of this SWNT varied less than 0.4% over a length of 6 mm.

A rectifying behaviour was found across an S–S intramolecular junction. With the aid of Raman positioning, four 50-nm-thick Pd electrodes were deposited 4 μm apart at desired positions along a SWNT with an S–S junction using a technique involving electron beam lithography, electron beam deposition and lift-off. Figure 3a shows an AFM image and a schematic diagram of the positions of the S–S junction and Pd electrodes. As the Pd–nanotube contact is ohmic in nature[4], the measured current–voltage, I–V, curves are not affected by the contact barrier. The I_{ds}–V_{ds} (drain-source current versus drain-source bias voltage) curves of segments S_1 and S_2 were symmetric and the current of segment S_2 was larger than that of segment S_1 at the same bias and gate voltages (Fig. 3b).

©2007 Nature Publishing Group

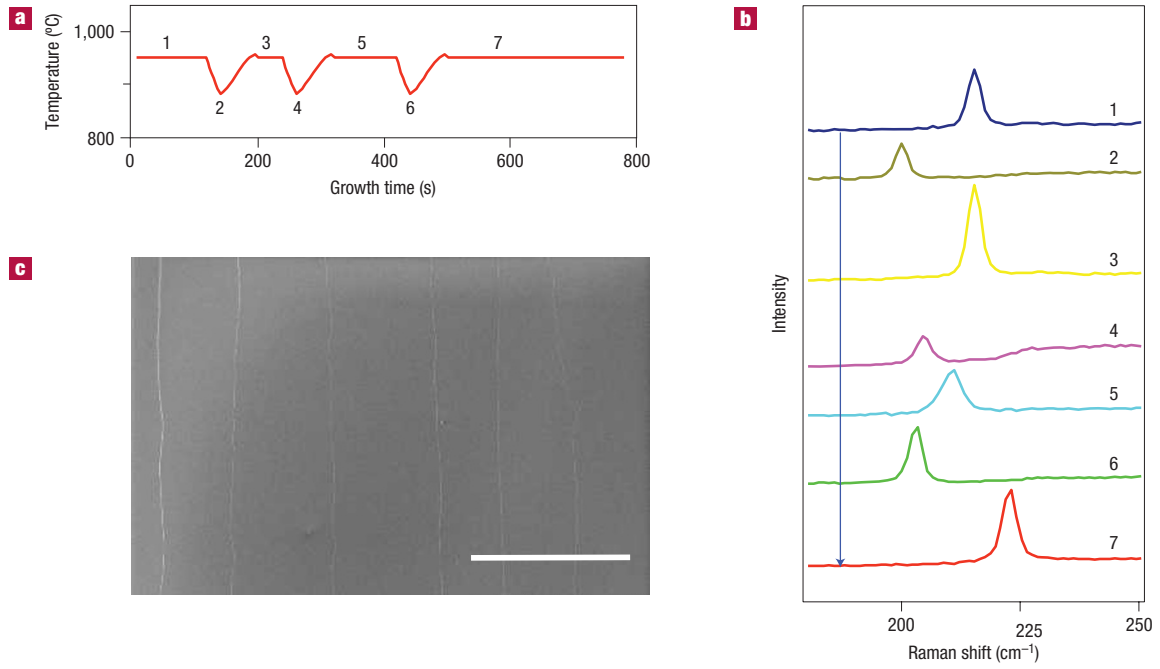

Figure 2 Six intramolecular junctions were induced by three temperature oscillations between 950 and 880 °C during CVD. a, Scheme of temperature oscillation with time. **b**, Raman RBM peak positions along a SWNT, each peak corresponds to a time period in **a**. More information is shown in Supplementary Information, Fig. S6. **c**, An SEM image of several parallel ultralong SWNTs grown during the temperature oscillation. The scale bar is 100 μm.

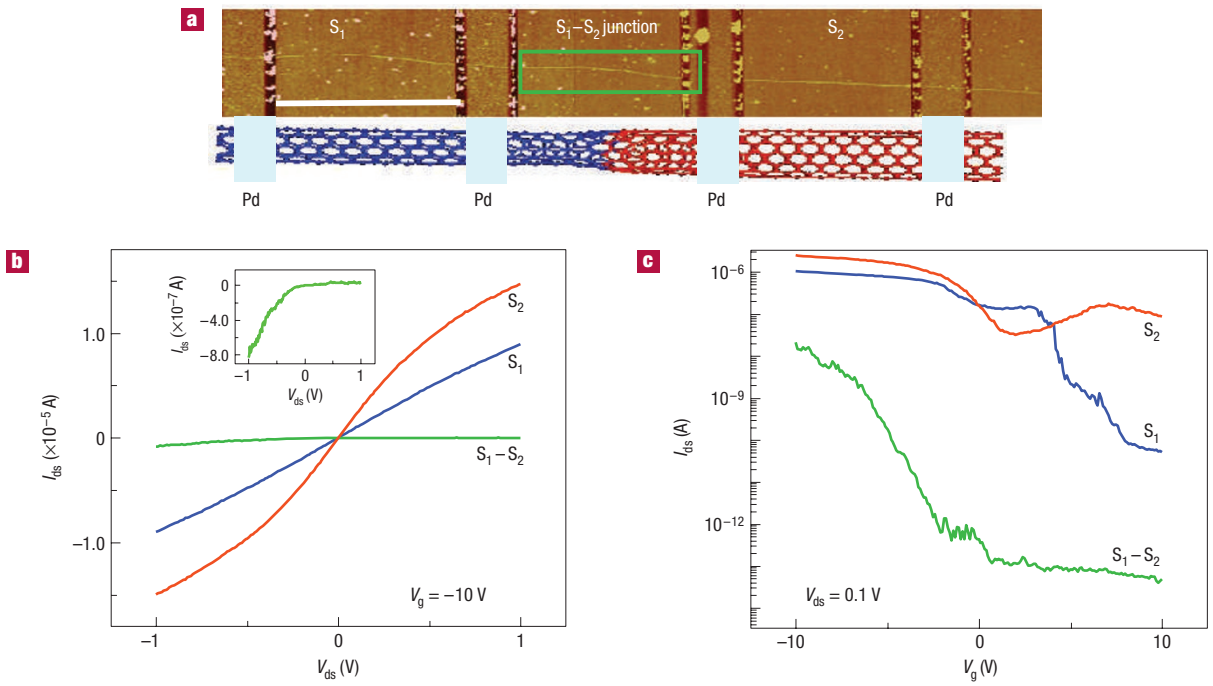

Figure 3 AFM image and electrical properties of an SWNT with an S–S intramolecular junction. a, An AFM image and a schematic diagram of an SWNT with an S–S intramolecular junction connected with four Pd electrodes. The scale bar is 4 μm. An AFM image of the diameter variation is shown in Supplementary Information, Fig. S5. **b**,**c**, I_{ds}–V_{ds} (**b**) and I_{ds}–V_g (**c**) curves of the three SWNT segments shown in **a**. The inset in **b** shows the rectifying behaviour of the intramolecular junction.

In contrast, the I_{ds}–V_{ds} curves across the junction (S_1–S_2) showed an asymmetric and rectifying behaviour (Fig. 3b, inset), and the rectification ratio (RR = current at −1 V/current at +1 V) was ~24. Figure 3c shows that the three segments of the nanotube showed different gate-voltage dependence. The on–off current ratios in segments S_1, S_1–S_2 and S_2 were 2.0×10^4, 4.9×10^5 and 75,

©2007 Nature Publishing Group

respectively. From the differences in the on-state current and the on–off current ratio, we can infer that the bandgap in segment S_1 was larger than the bandgap in segment S_2. The rectifying behaviour was caused by the barrier formed at the interface of two different semiconducting nanotubes with different bandgaps.

It is well accepted that the size of a catalyst particle determines the diameter of the nanotube[16]. However, in this study, we observed for the first time that even with the same catalyst particle, the diameter of a SWNT may vary with changing temperature. Specifically, higher temperature leads to thinner SWNTs with the same catalyst particle, and vice versa. The ultralong SWNTs are believed to grow via the tip-growth mechanism[17], in which the growing end of the SWNT and the catalyst float above the substrate. Ethanol molecules dissociate on the surface of the catalyst particle, releasing active carbon atoms that dissolve into the catalyst and precipitate to form a tubular SWNT. The nanotube diameter is largely controlled by the size of the catalyst particle, and remains uniform under a constant temperature. However, if the temperature changes during the growth of a SWNT, the shape of the catalyst particle may change owing to the change of the carbon solubility in the catalyst and the change of the interfacial energy between the catalyst and the SWNT. In addition, a SWNT can be viewed as a rolled-up seamless graphene sheet. Smaller diameter leads to higher strain energy in the wall of the SWNT[18,19]. Higher temperature reduced the stiffness of the graphene sheet and consequently favours the formation of smaller SWNTs.

We also found that statistically most intramolecular junctions are S–S type or M–M type. Only a small fraction ($<5\%$) of the junctions investigated here are S–M or M–S type. This observation indicates a potential possibility to selectively grow SWNTs with desired conducting properties. Further study is under way to investigate the mechanism for this observation.

In summary, we have discovered an effective method, temperature variation, to grow SWNTs with intramolecular junctions in a controlled way. This is achieved due to a phenomenon observed for the first time in this study: the diameter of a growing SWNT becomes smaller at higher temperature, and vice versa, even though the catalyst particle at the growing tip remains the same. Intramolecular junctions in SWNTs reported previously were formed mostly coincidentally without any control[2,5–8]. Using the strategy reported here, it is feasible to grow SWNT intramolecular junctions at designated places and to grow arrays of junctions by heating the substrate locally using infrared light during CVD in a way similar to lithography. This is the first step towards developing next-generation, carbon-nanotube based devices and circuits, such as field-effect transistors, sensors, nanoelectromechanical systems and so on.

Received 8 November 2006; accepted 1 February 2007; published 18 March 2007.

References

1. McEuen, P. L. Nanotechnology—Carbon-based electronics. *Nature* **393**, 15–17 (1998).
2. Yao, Z., Postma, H. W. C., Balents, L. & Dekker, C. Carbon nanotube intramolecular junctions. *Nature* **402**, 273–276 (1999).
3. Baughman, R. H., Zakhidov, A. A. & de Heer, W. A. Carbon nanotubes—The route toward applications. *Science* **297**, 787–792 (2002).
4. Javey, A., Guo, J., Wang, Q., Lundstrom, M. & Dai, H. J. Ballistic carbon nanotube field-effect transistors. *Nature* **424**, 654–657 (2003).
5. Ho, G. W., Wee, A. T. S. & Lin, J. Electric field-induced carbon nanotube junction formation. *Appl. Phys. Lett.* **79**, 260–262 (2001).
6. Yudasaka, M., Ichihashi, T., Kasuya, D., Kataura, H. & Iijima, S. Structure changes of single-wall carbon nanotubes and single-wall carbon nanohorns caused by heat treatment. *Carbon* **41**, 1273–1280 (2003).
7. Doorn, S. K. *et al.* Raman spectral imaging of a carbon nanotube intramolecular junction. *Phys. Rev. Lett.* **94**, 016802 (2005).
8. Doorn, S. K. *et al.* Raman spectroscopy and imaging of ultralong carbon nanotubes. *J. Phys. Chem. B* **109**, 3751–3758 (2005).
9. Zheng, L. X. *et al.* Ultralong single-wall carbon nanotubes. *Nature Mater.* **3**, 673–676 (2004).
10. Zhang, Y., Zhang, J., Son, H., Kong, J. & Liu, Z. Substrate-induced Raman frequency variation for single-walled carbon nanotubes. *J. Am. Chem. Soc.* **127**, 17156–17157 (2005).
11. Huang, L. *et al.* Cobalt ultrathin film catalyzed ethanol chemical vapor deposition of single-walled carbon nanotubes. *J. Phys. Chem. B* **110**, 11103–11109 (2006).
12. Dresselhaus, M. S., Dresselhaus, G., Jorio, A., Souza, A. G. & Saito, R. Raman spectroscopy on isolated single wall carbon nanotubes. *Carbon* **40**, 2043–2061 (2002).
13. Kataura, H. *et al.* Optical properties of single-wall carbon nanotubes. *Synth. Met.* **103**, 2555–2558 (1999).
14. Jorio, A. *et al.* Structural (n, m) determination of isolated single-wall carbon nanotubes by resonant Raman scattering. *Phys. Rev. Lett.* **86**, 1118–1121 (2001).
15. White, C. T. & Mintmire, J. W. Fundamental properties of single-wall carbon nanotubes. *J. Phys. Chem. B* **109**, 52–65 (2005).
16. Liao, X. Z. *et al.* Effect of catalyst composition on carbon nanotube growth. *Appl. Phys. Lett.* **82**, 2694–2696 (2003).
17. Huang, S. M., Woodson, M., Smalley, R. & Liu, J. Growth mechanism of oriented long single walled carbon nanotubes using "fast-heating" chemical vapor deposition process. *Nano Lett.* **4**, 1025–1028 (2004).
18. Hernandez, E., Goze, C., Bernier, P. & Rubio, A. Elastic properties of single-wall nanotubes. *Appl. Phys. A* **68**, 287–292 (1999).
19. Li, Y. *et al.* On the origin of preferential growth of semiconducting single-walled carbon nanotubes. *J. Phys. Chem. B* **109**, 6968–6971 (2005).
20. Melchor, S. & Dobado, J. A. CoNTub: An algorithm for connecting two arbitrary carbon nanotubes. *J. Chem. Inf. Comput. Sci.* **44**, 1639–1646 (2004).

Acknowledgements

This work was supported by NSFC (20573002, 20673004, 50521201) and MOST (2006CB932701, 2006CB932403).
Correspondence and requests for materials should be addressed to J.Z. or Z.L.
Supplementary Information accompanies this paper on www.nature.com/naturematerials.

Competing financial interests

The authors declare no competing financial interests.

Reprints and permission information is available online at http://npg.nature.com/reprintsandpermissions/

©2007 Nature Publishing Group